

Misalignments characterization in micro-CPV modules with deep learning compared with electrical performance parameters

Cite as: AIP Conference Proceedings 2550, 030005 (2022); <https://doi.org/10.1063/5.0100320>
Published Online: 02 September 2022

 Luis San José,  Guido Vallerotto,  Rebeca Herrero, et al.



View Online



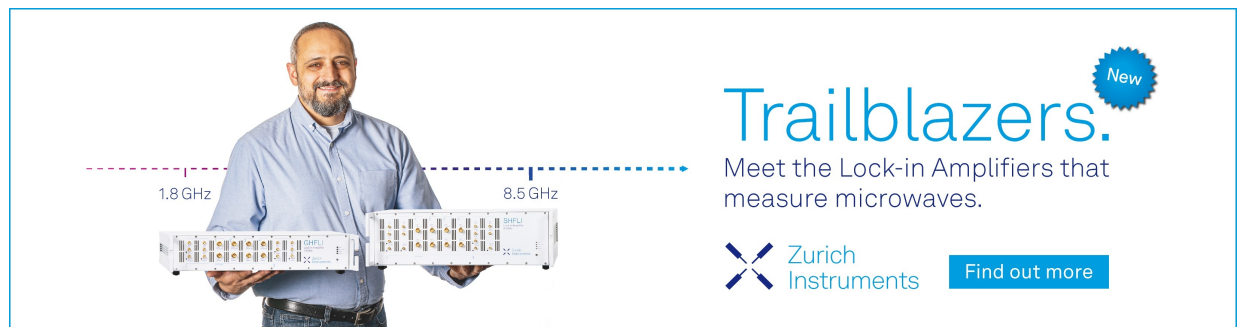
Export Citation


ARTICLES YOU MAY BE INTERESTED IN

HIPERION: Scale-up of hybrid planar micro-tracking solar panels for rooftop compatible CPV
AIP Conference Proceedings 2550, 030001 (2022); <https://doi.org/10.1063/5.0101843>


Solar simulator for indoor characterization of hybrid CPV/flat-plate modules
AIP Conference Proceedings 2550, 020001 (2022); <https://doi.org/10.1063/5.0102699>

Humidity characterization and control in planar micro-tracking CPV modules
AIP Conference Proceedings 2550, 030003 (2022); <https://doi.org/10.1063/5.0099320>



Trailblazers. 

Meet the Lock-in Amplifiers that measure microwaves.

 Zurich Instruments [Find out more](#)

Misalignments Characterization in Micro-CPV Modules with Deep Learning Compared with Electrical Performance Parameters

Luis San José^{a)}, Guido Vallerotto, Rebeca Herrero, and Ignacio Antón

*Instituto de Energía Solar, Universidad Politécnica de Madrid
Avda/Complutense 30, 2040 Madrid, Spain*

^{a)}Corresponding author: luis.sanjose@ies.upm.es

Abstract. A method for misalignments characterization through image acquisition has been adapted and applied to micro-CPV. For this purpose, a measurement set-up and an image processing are proposed and explained. Two different image processing are explored: one based on conventional segmentation method, and another based on Deep Learning. The method is validated based on two measurements that determine the accuracy and the repeatability, showing that the processing based on Deep Learning improves both measurement parameters.

INTRODUCTION

Micro-CPV (Concentrator Photovoltaics) uses sub-scaled lenses and receivers (*i.e.*, Secondary Optical Element (SOE) plus solar cell) in comparison with conventional CPV, pursuing a material consumption reduction as a cost-effective way for competing against conventional photovoltaics price [1]. Because of the size reduction in the optical components, novel thicker lenses may be used in exchange for higher angular tolerances than the conventional CPV lenses [2]. If these novel lenses concentrate sunlight into a spot for an angular range similar to the sunlight angle of incidence variation along the day, an on-axis concentration can be achieved by only displacing the receivers' plane with respect the lenses array plane. This concept, known as integrated tracking [3], dispenses with placing the modules onto a mechanical tracker. The main advantage of this, is not only to avoid the costs of a tracker system that points the modules towards the sun, but also the possibility of micro-CPV modules architectural integration on rooftops.

However, the small sizes of micro-CPV components (and additionally the integrated tracking system) require positioning tolerances between the lenses and the receivers very tight. If there are misplacements between them, the module current-voltage (I-V) curve will show a worse FF that will reduce the output power, and consequently, the efficiency. A proper misalignments characterization among lens-receiver units that compose a module during its manufacturing process or development stage, will allow correcting these misplacements and reducing its effect on the electrical behavior.

In this regard, the luminescence inverse method [4,5] was proposed and later implemented in the so-called Module Optical Analyzer [6,7] for the analysis of CPV modules in a production line [8,9]. The method was conceived to be integrated with a CPV solar simulator [10,11], since the use of a collimator mirror is mandatory. However, the resolution achieved is not suitable for a micro-CPV module with lens area of hardly two square centimeters.

In this work, an alternative method for characterizing misalignments in CPV based on image acquisition is applied. The method, validated in previous works [12] by measuring misalignments between the lens-receiver units of a module [13] or between modules mounted on a tracker [14], is based on taking a photograph of each receiver that composes a module magnified through its corresponding lens. Differences between the receiver and the lens aperture centers in the images are translatable into degrees based on simulations or through experimental constants.

The goal of this work is to apply the cited method for measuring the misalignments in a micro-CPV module with integrated tracking. For this purpose, the peculiarities of applying the method to micro-CPV are explained, and a

measurement set up is proposed along with an image processing for a precise detection of the lens and the receiver. The method is validated through two measurements for determining the precision and the repeatability, where an image processing based on Deep Learning improves the receiver detection with respect to a conventional processing.

APPLICATION TO MICRO-CPV: CASE STUDY

A novel micro CPV Insolight module with integrated tracking has been used for applying the misalignments characterization method. The module is composed by 1mm square MJ solar cells with semispherical SOEs attached to them. The Primary Optical Element is a biconvex 8.34 mm side hexagonal lens. For performing an integrated tracking, the receivers' plane is displaced through mechanical actuators in X, Y and Z direction with a maximum travel of ± 12 mm in XY. To apply the method to micro-CPV modules, some considerations must be done. On one hand, to measure the misplacements between the optical elements with enough precision, a high resolution, (*i.e.*, high ratio of pixels per millimeter on the image) is needed, since receiver misplacements of 0.1mm implies misalignments of $\sim 0.5^\circ$. On the other hand, since one image per lens-receiver unit is required, and the camera position with respect to the optical unit affects to the measured misalignment, the camera positioning must be accurately controlled. Moreover, the novel lenses used in the module are anidolic optics (Fig.1.b), that is, the receiver shape will be deformed when observed from an off-axis position. Therefore, the receiver shape results deformed if the camera is not centered with respect to the unit under examination. In this scenario, the processing gets more complicated and additional errors may be introduced when detecting receiver and lens position in the image. In this sense, the images must be treated for obtaining the lens and the receiver position with enough precision (*e.g.*, in a 1mm size receiver imaging under a resolution of 300px/mm an error of 5px implies an error of $\sim 0.05^\circ$).

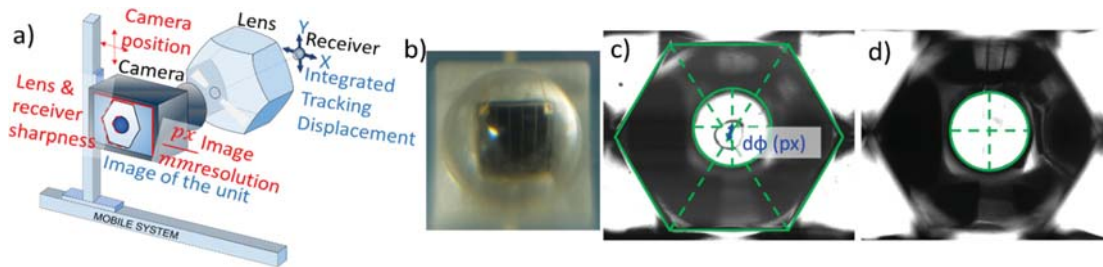


FIGURE 1. a) Set up proposed for achieving an accurate camera positioning; b) micro-CPV anidolic optics deform the receiver shape when observed through it; c) and d) image focusing to the lens and to the receiver respectively.

The set-up and characterization method developed consist of the following components and characteristics:

- A macro lens focus has been used in the camera to achieve a high-resolution image.
- The camera has been mounted on a XYZ translation stage with micrometric precision, with a position uncertainty below $13 \mu\text{m}$.
- The image acquisition is performed with the module under electroluminescence conditions to get an image of the lens and the receiver with sharper edges (Fig.1.c and d).
- The image processing is based on Deep Learning, to improve the detection in the position of the receiver.
- Moreover, since the misalignment is measured as the difference between each receiver center and its corresponding lens center (Fig.1.c and d), the used macro lens introduces an additional difficulty: getting closer to the module lens array plane implies not having a single focus position for seeing clearly both elements. In consequence, two pictures (one focusing to the lens and another focusing to the receiver) are taken for determining the misalignment of one optical unit.

IMAGE PROCESSING

As explained above, one key aspect in the method application to micro-CPV is to reach a precise detection of both the lens and the receiver, which is accomplished by using an image processing developed in Matlab for automatically obtain both elements' centers. For this, two different image processing have been developed with similar schemes; one aimed to detect the center of the receiver circular shape, and other aimed to detect the hexagonal edges of the lens aperture. Both have three stages with clearly different purposes: the first step is a preprocessing addressed to enhance

the features of interest in the images (areas and edges). A second step is the segmentation where the shapes of the lens/receiver are extracted and discerned from the rest of the image. Finally, a third step is the detection where image-processing algorithms find a unique position of the lens and the receiver centers. In the case of the receivers' images, the segmentation stage has been carried out in two ways: with a conventional processing and using Deep Learning.

Receiver Image Processing

Pre-Processing

The pre-processing of the receiver image is aimed at boosting the contrast between the clear circular receiver area and the background of the image, making both more homogeneous collaterally. Several utilities of the Matlab Image Processing Toolbox have been applied in this step. First, a median filter is applied (Fig.2.b), removing the sensor noise and possible shines from the lens on the image. Then, a Local Laplacian Filter (LLF) increases the contrast between the dark and the bright areas, preserving strong edges (zones where gray level changes abruptly) and homogenizing areas (Fig.2.c). A local contrast adjustment performed right after the LLF improves the gray level separation between the receiver and the background and removes shades from the cell fingers or from the lens fixing point to the glass substrate (the little dark circle observed) (Fig.2.d). At this point, a multi-thresholding allows quantifying and distinguishing the 255 levels of gray in 7 different groups (Fig.2.e). For these groups, a contrast adjustment and gray-leveling is applied at pixel level, adding a proportional brightness to the pixel if it belongs to the two brightest groups or subtracting brightness if it belongs to the two darkest groups. For the intermediate gray levels, a less severe correction is applied in function of the group and the pixel gray level. As a result of the pre-processing, the receiver is well contrasted and presents a brighter and more homogeneous area than in the original image (Fig.2.f).

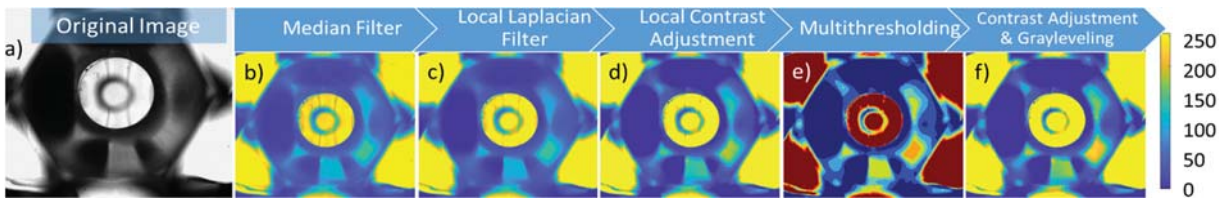


FIGURE 2. Receiver image pre-processing steps, where image gray-levels are represented in colormaps as indicated on the right.

Segmentation

The goal of this part of the image processing must be to correctly extract the receiver area for a later detection. For achieving this, a conventional processing based on the Superpixels Oversegmentation (SPO) [15] can be used to extract the circular area. The SPO groups the image pixels into regions using the grayscale level and the spatial proximity as parameters. After this, a multi-thresholding discerns the receiver area and morphological operations help to refine the segmented area, completing missing edges.

Alternatively, the Matlab Computer Vision and Deep Learning Toolboxes may be used for the segmentation, so by training a pre-trained Convolutional Neural Network (CNN), a semantic segmentation network based on Deep Learning (DL) labels the image pixels of the receiver and separate them from the background. A Convolutional Neural Network is a machine learning algorithm for classifying objects in images composed by multiple layers of convolutional bi-dimensional filters. Since there is an extent state of the art of CNN, a strategy usually followed is to modify a pre-existent CNN configuration (*i.e.*, pre-trained), adapting the layers and filter sizes to the input images desired. The semantic segmentation consists of clustering the parts of an image belonging to a same object through a CNN, linking each pixel in the image to an object category (in this case to receiver or to background categories) [16].

For creating a semantic segmentation network suitable for the used image sizes (2201x2201 pixels with 16 bits of monochrome depth), an existent pre-trained network is re-adapted. The network is composed by a stacking of down-sampling layers followed by ReLU (Rectified Linear Units), convolutional and up-sampling layers, and ending with a final classification layer. This pile of layers is aimed at either, transforming the image and preparing some of its characteristics to be learned for a good labelling, or at learning the desirable characteristics for the classification output label. The down-sampling layers reduce the amount of information contained in the images (by re-escalations, geometrical transformations, rotations...), whereas the ReLU layers are the true neurons (the activation functions) of the neural network, where the learning occurs in each iteration. The ReLU layers serve during the CNN training to

account for interaction and non-linear effects in the features of the images that will help to correctly identify the receiver area (in this particular case). Thus, during the training, these layers adjust their activation parameters (input weights) in function of the relevant features to reach the desired labelling. In the end, the up-sampling layers enlarge the image size and labelling information to meet the input sizes.

Once the architecture of the CNN is defined and adapted, a training where the CNN adjusts the weights of the ReLU layers, “learning” about the desired output classification, must be done. For doing this with the receiver image, a training of the CNN must be carried out using as input a set of labelled receiver images; this data set can never belong to the set of images that are meant to be processed. Thus, 25 images from previous measurements of the module have been manually labelled, discerning the receiver area and the background using the Matlab Image Labeller application for this purpose. With the 25 images training set and the described customized semantic segmentation network, the network has been trained iteratively until the precision (intended as the coincidence ratio between the manually segmented areas and the areas segmented automatically by the CNN) indicated a value above 90%. The trained network performance has been evaluated with another set of 56 images, which belong to a different measurement of the same module. This process has permitted to check visually that the precision reached by the training process allows correctly detecting the receiver areas in the images (Fig.3).

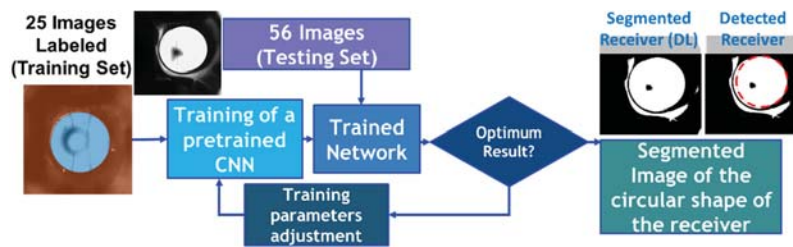


FIGURE 3. Scheme of the training process followed for applying Deep Learning to the receiver segmentation.

Detection

With the image of the segmented receiver the Hough transform applied for circles [17] finds the receiver center by calculating the most probable existing circle in the image. This circle center is given as the maximum value of an accumulator (of the same size as the image) filled by the algorithm, where each edge pixel casts votes around a circle of a given radius. Because the segmentation reached through DL is good enough, and a low sensitivity value is set (as input parameter in the Hough transform) a unique circle in the image is detected in the image (Fig.3 right).

Lens Image Processing

Pre-Processing

The pre-processing applied for the lens image is very similar to the one applied to the receiver image: a median filter reduces the noise in the image and homogenizes the different areas (Fig.4.b) and a following LLF increases the contrast and enhances the lenses edges (Fig.4.c). Then, a local contrast adjustment separates the gray levels, increasing the edges differentiation. However, as the aim of this pre-processing is to enhance the hexagon edges instead of an area, in place of applying a multi-thresholding and a gray-leveling, a sharpening step is introduced for increasing and maximizing the gradient differences of the image edges (Fig.4.d).

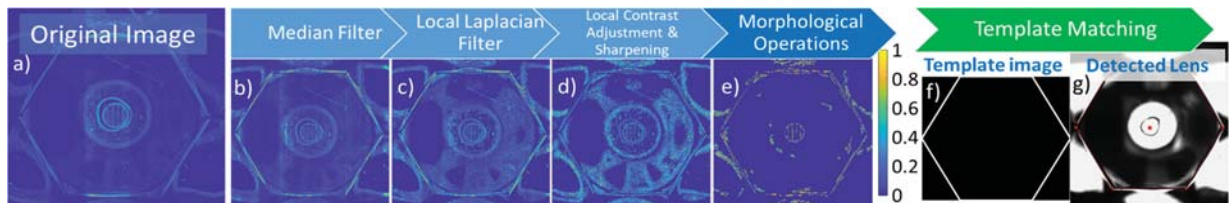


FIGURE 4. a) to d) pre-processing and segmentation e) of the lens image, where the gradient of the images in each step is represented scaled in colormaps as indicated. With a hexagonal template f) the template matching finds the lens center g).

Segmentation

Using the gradient of the pre-processed image a binary image is obtained. Since the lens edges have a continuous gradient with a particular orientation in the image, using linear structure elements with the same orientation as the edges for performing an erosion, the edges of the lens aperture are well extracted (Fig.4.e).

Detection

At last, using the template matching algorithm [18], the lens center is detected. This detection is done using a template (Fig.4.f) consisting of a hexagon with the same dimensions as the lenses' aperture in the images. The template matching algorithm fills an accumulator with the results of the normalized cross correlation (NCC) obtained in each position of the image where the template might fit. The point with the highest value of the accumulator is where a hexagonal shape is more likely to be found and thus it is pointed as the center of the lens (Fig.4.g).

VALIDATION OF THE METHOD THROUGH ACCURACY AND REPEATABILITY MEASUREMENTS

The measurement method has been validated through two experiments for determining the method's uncertainty and repeatability:

- Firstly, known misalignments have been introduced and measured with the method to evaluate the uncertainty.
- Secondly, the proposed measurement has been carried out several times for a single unit (with a given known misalignment) under different camera positions to evaluate the repeatability.

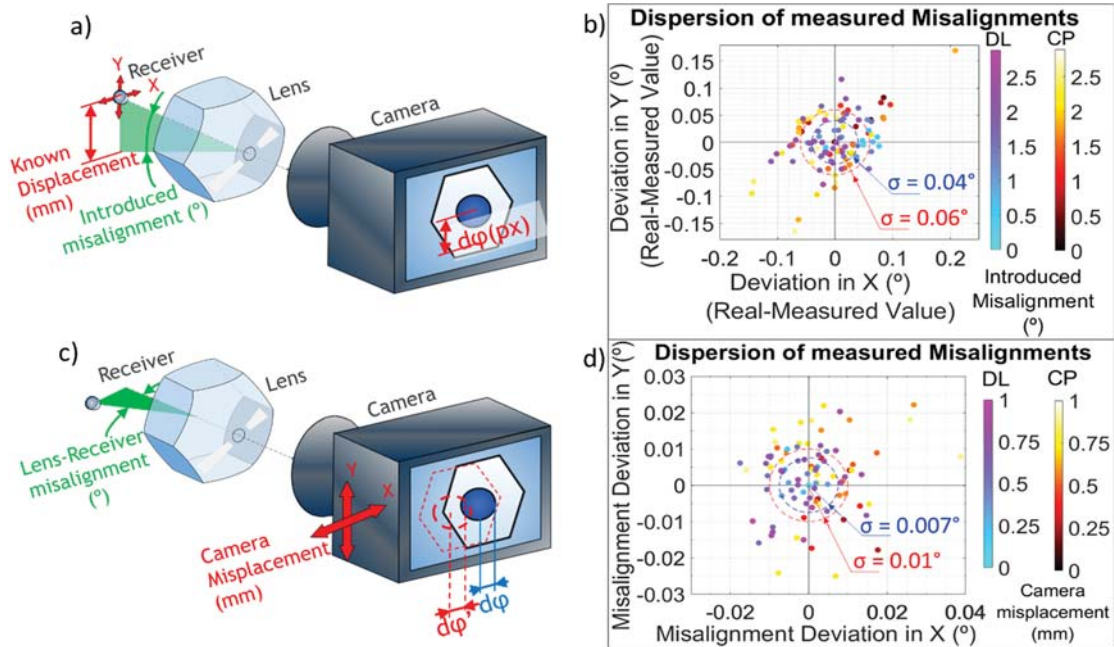


FIGURE 5. a) Measurement scheme for accuracy determination. b) Deviations from real value of misalignment obtained through DL and conventional processing (CP). c) Measurement scheme for repeatability determination. d) Deviations in the misalignment measured in each XY position of the camera for both processing methods (DL and CP).

To determine the uncertainty of the receiver detection in the measured misalignment, the integrated tracking system has been set via software in different positions consisting of steps of 0.1mm with a travel of $\pm 0.4\text{mm}$ ($\sim \pm 2.7^\circ$) in XY direction (introducing known receiver displacements). For each set receiver position, a picture of a unique lens-receiver unit has been acquired and the misalignment has been determined by the proposed method (see Figure 5.a).

In the presented case study, misalignments are produced by misplacements of the receivers (in mm), introduced purposely with the integrated tracking displacement. This displacement can be translated into degrees through an

experimental calibration or theoretically (by knowing the dimensions and characteristics of the optic system), equivalating these associated degrees to the pointing vector of the lens-receiver unit compared with an ideally aligned one. The different pointing vectors, that is, the different misalignments of the module units will impact in the angular-optical behavior of the system, usually characterized by the Angular Transmission Function (ATF).

Thus, deviations between the real introduced misalignments (checked out during the experiment by precisely measuring the introduced offset in the receivers' plane) and the measured ones (using the image-based method) will give an uncertainty linked to the image processing (*i.e.*, the imprecision in the receiver and the lens detection).

On the other side, uncertainty associated to the camera position (how centered is compared to the micro-CPV lens) has been determined by measuring the misalignment of a lens-receiver unit displacing the camera to different positions around the lens center, using for this the cartesian XYZ system where the camera is attached. The camera has been displaced with steps of 0.2mm and a travel of ± 1 mm with respect to the lens center, and images focusing to the lens and to the receiver have been acquired in each position (Fig.5.c). Since the misalignment between the lens and the receiver in the examined unit is constant (*i.e.*, the receiver position is not modified), the differences in the misalignment measured in each position (where the camera has been placed) will give an idea of the corresponding uncertainty (*i.e.*, the method repeatability) that takes place when the measurement conditions slightly vary.

To quantify the improvement that the DL processing supposes to the receiver detection with respect to the conventional image processing [19], the images of both experiments (accuracy and repeatability) have been processed with the two image process methods, and the results have been compared (Fig.5.b and d). In each graph, the standard deviation of the errors distribution in each measurement is indicated as a circle centered in 0,0. The deviations for both measurements are represented color-mapped in function to the associated magnitude under which the measurement has been performed (introduced misalignment in the case of the accuracy measurement, and camera displacement in the case of the repeatability measurement). With the proposed method, the standard deviation of the errors committed on the measured misalignment related to the receiver detection are 0.06° for the conventional image processing and 0.04° for the DL-based processing (Fig.5.b). The errors are defined as the deviations between the real misalignment value (*i.e.*, the introduced displacement of the receiver transformed into degrees), and the value measured through the images. As indicated in the graph, the introduced displacements represent misalignments of up to 2.79° . For both processing techniques the error committed is very low, but it can be noted how the accuracy improves with the DL. The standard deviation of the errors committed on the measured misalignment related to the camera position are 0.01° using conventional processing and 0.007° using DL based processing (Fig.5.d); a very low value for the intended measurement. The errors are defined as the differences between the misalignment measured when the camera optical axis coincides with the lens axis (*i.e.*, camera displacement is zero), and the misalignment measured in each position where camera is displaced.

With both measurements, the obtained results confirm the method applicability to micro-CPV with a bounded uncertainty linked to the detection accuracy and a repeatability given by the measurement set-up and the image processing. Besides, DL processing techniques applied to receiver detection improves both measurement parameters.

MISALIGNMENTS MEASUREMENT VS ELECTRICAL MEASUREMENT

Once the method characterization was performed through the validation measurements above explained, it can be applied for micro-CPV modules misalignments characterization. A misalignment characterization, along with an electrical measurement, such as the I-V curve, can give a valuable module diagnosis. In the case that a degradation of the module I-V curve is observed, it can be attributed to the dispersion of the measured misalignments and to the system angular acceptance. This will allow not only to explore the causes of electrical performance issues, but to give feedback of the module assembly manufacturing process or the mechanical tolerances required for an optimum module behavior in terms of the integrated tracking system.

CONCLUSIONS

A method based on image acquisition for CPV misalignments characterization has been applied successfully to micro-CPV modules. Two experiments were carried out to determine the main sources of uncertainty, providing an accuracy of $\pm 0.04^\circ$ and repeatability of $\pm 0.007^\circ$ with DL-based processing respectively. A robust image processing is needed for reaching these acceptable uncertainties in the measurement, where Deep Learning techniques have shown a clear improvement with respect to the conventional processing presented in previous works.

ACKNOWLEDGMENTS

The research leading to these results has received funding from the European Commission H2020 under the HIPERION project (857775). We also acknowledge the support received by the Spanish Ministerio de Ciencia, Innovación y Universidades- Agencia Estatal de Investigación, under Micro-PV project (ENE2017-87825-C2-1-R).

REFERENCES

1. C. Domínguez et al., "A review of the promises and challenges of micro-concentrator photovoltaics." *AIP Conference Proceedings*. Vol. 1881. No. 1. AIP Publishing, 2017.
2. M. Wiesenfarth, I. Anton, and A. W. Bett. "Challenges in the design of concentrator photovoltaic (CPV) modules to achieve highest efficiencies." *Applied Physics Reviews* 5.4 (2018): 041601.
3. G. Nardin et al. "Industrialization of hybrid Si/III–V and translucent planar micro-tracking modules." *Progress in Photovoltaics: Research and Applications*.
4. R. Herrero, C. Domínguez, S. Askins, I. Antón, and G. Sala, "Two-dimensional angular transmission characterization of CPV modules," *Opt. Express* 18(S4), A499–A505 (2010).
5. R. Herrero, C. Domínguez, S. Askins, I. Antón, and G. Sala, "Luminescence inverse method for CPV optical characterization," *Opt. Express* 21(S6), A1028–A1034 (2013).
6. R. Herrero et al., "Module optical analyzer: Identification of defects on the production line". In *AIP Conference Proceedings* (Vol. 1616, No. 1, pp. 119-123). American Institute of Physics, 2014.
7. R. Herrero et al., "Evaluation of Misalignments within a Concentrator Photovoltaic Module by the Module Optical Analyzer: A Case of Study Concerning Temperature Effects on the Module Performance," *Jpn. J. Appl. Phys.* 54(8S1), 08KE08 (2015).
8. R. Herrero et al., "Experimental Analysis and Simulation of a Production Line for CPV Modules: Impact of Defects, Misalignments, and Binning of Receivers," *Energy Sci. Eng.* 5(5), 257–269 (2017).
9. R. Herrero, S. Askins, I. Antón, G. Sala, K. Araki, and H. Nagai, "Module optical analyzer: Identification of defects on the production line," (2014) *AIP Conference Proceedings*, 1616, pp. 119–123.
10. C. Domínguez, I. Antón, and G. Sala, "Solar simulator for concentrator photovoltaic systems," *Opt. Express* 16(19),14894–14901 (2008).
11. I. Antón, C. Domínguez, M. Victoria, R. Herrero, S. Askins, G. Sala, "Characterization Capabilities of Solar Simulators for Concentrator Photovoltaic Modules." *Jpn. J. Appl. Phys.* 51 10ND12 (2012).
12. L. San José, G. Vallerotto, R. Herrero, and I. Antón, "Misalignments measurement of CPV optical components through image acquisition," *Opt. Express* 28, 15652-15662 (2020).
13. L. San José et al. (2018, September). "Computer vision algorithm for relative misalignments estimation in CPV modules". In *AIP Conference Proceedings* (Vol. 2012, No. 1, p. 100004). AIP Publishing LLC.
14. L. San José, R. Herrero, & I. Antón, "Relative misalignments estimation in on-tracker CPV modules through image processing". In *AIP Conference Proceedings*. Vol. 2149, No. 1. AIP Publishing, 2019.
15. R. Achanta et al. "SLIC superpixels compared to state-of-the-art superpixel methods." *IEEE transactions on pattern analysis and machine intelligence* 34.11 (2012): 2274-2282.
16. L. Chen et al. (2018). DeepLab: Semantic image segmentation with deep convolutional nets, atrous convolution, and fully connected CRFs. *IEEE Transactions on Pattern Analysis and Machine Intelligence*, 40(4), 834-848. doi:10.1109/TPAMI.2017.2699184
17. H.K Yuen, J. Princen, J. Illingworth, and J. Kittler. "Comparative study of Hough transform methods for circle finding." *Image and Vision Computing*. Volume 8, Number 1, 1990, pp. 71–77.
18. K. Briechele, and U.D. Hanebeck. "Template matching using fast normalized cross correlation." *Optical Pattern Recognition XII*. Vol. 4387. International Society for Optics and Photonics, 2001.
19. L. San José, G. Vallerotto, R. Herrero, and I. Antón, "Misalignments Characterization for Micro-CPV Modules" (to be published) *AIP Conference Proceedings* MS ID: AIPCP20-AR-CPV16-00015 (2020).